Am J Physiol Heart Circ Physiol 283: H598–H605, 2002.
First published April 11, 2002; 10.1152/ajpheart.00198.2002.

H_2O_2-induced Ca^{2+} overload in NRVM involves ERK1/2 MAP kinases: role for an NHE-1-dependent pathway

EMILY C. ROTHSTEIN,[1] KENNETH L. BYRON,[2] RYAN E. REED,[1]
LARRY FLIEGEL,[3] AND PAMELA A. LUCCHESI[1]
[1]*Department of Physiology and Biophysics, University of Alabama at Birmingham, Birmingham, Alabama 35294;* [2]*Department of Medicine and the Cardiovascular Institute, Loyola University Chicago, Maywood, Illinois 60153; and Department of Biochemistry, University of Alberta Edmonton, Edmonton, Alberta, Canada T6G 2H7*

Received 6 March 2002; accepted in final form 5 April 2002

Rothstein, Emily C., Kenneth L. Byron, Ryan E. Reed, Larry Fliegel, and Pamela A. Lucchesi. H_2O_2-induced Ca^{2+} overload in NRVM involves ERK1/2 MAP kinases: role for an NHE-1-dependent pathway. *Am J Physiol Heart Circ Physiol* 283: H598–H605, 2002. First published April 11, 2002; 10.1152/ajpheart.00198.2002.—Generation of reactive oxygen species (ROS) and intracellular Ca^{2+} overload are key mechanisms involved in ischemia-reperfusion (I/R)-induced myocardial injury. The relationship between I/R injury and Ca^{2+} overload has not been fully characterized. The increase in Na^+/H^+ exchanger (NHE-1) activity observed during I/R injury is an attractive candidate to link increased ROS production with Ca^{2+} overload. We have shown that low doses of H_2O_2 increase NHE-1 activity in an extracellular signal-regulated kinase (ERK)-dependent manner. In this study, we examined the effect of low doses of H_2O_2 on intracellular Ca^{2+} in fura 2-loaded, spontaneously contracting neonatal rat ventricular myocytes. H_2O_2 induced a time- and concentration-dependent increase in diastolic intracellular Ca^{2+} concentration that was blocked by inhibition of ERK1/2 activation with 5 μM U-0126 (88%) or inhibition of NHE-1 with 5 μM HOE-642 (50%). Increased NHE activity was associated with phosphorylation of the NHE-1 carboxyl tail that was blocked by U-0126. These results suggest that H_2O_2 induced Ca^{2+} overload is partially mediated by NHE-1 activation secondary to phosphorylation of NHE-1 by the ERK1/2 MAP kinase pathway.

ischemia-reperfusion; reactive oxygen species; myocardium

REPERFUSION of ischemic myocardium leads to myocardial stunning, which is characterized by changes in the myocardial metabolic and contractile states. Alterations in Ca^{2+} homeostasis and cardiac myofilament responsiveness to Ca^{2+} are thought to be responsible for the contractile dysfunction in the stunned myocardium. Cardiomyocyte cytosolic Ca^{2+} overload causes numerous potentially degenerative states, including alterations in Ca^{2+} transport processes, altered contraction, arrhythmogenesis, and cell death. It has been suggested that the burst in reactive oxygen species (ROS) on reperfusion may contribute to Ca^{2+} overload (14).

ROS are by-products of oxygen consumption that are easily managed under normal conditions with reactive oxygen scavengers (16, 26). Several forms of ROS are generated during I/R, including superoxide (O_2^-), H_2O_2, and the highly reactive hydroxyl radical (·OH). ROS have been demonstrated to cause lipid peroxidation and myocardial injury, and are thought to trigger the contractile dysfunction observed during reperfusion (9). Increased levels of ROS production have been shown in the isolated perfused rabbit heart peaking 10–30 s after reperfusion after an ischemic episode (41, 42). Scavengers of free radicals such as catalase and superoxide dismutase can reduce myocardial stunning and reperfusion arrhythmias (3). Finally, exposure of nonischemic myocardium or myocytes to ROS can produce cell injury similar to that seen in ischemia-reperfusion (I/R) (14).

Indirect measures of oxidant stress have also been studied in humans after myocardial I/R. For example, electron spin resonance has been used to show peak production of ROS at 5 and 25 min after reperfusion in patients undergoing coronary artery bypass graft surgery (10) and an increase in oxidative stress during transient ischemia in patients undergoing elective coronary angioplasty (6).

The cellular mechanisms of oxidant injury and its relationship to Ca^{2+} overload in the cardiomyocyte have not been elucidated. High concentrations of H_2O_2 (1–10 mM) have been shown to produce Ca^{2+} overload via regulation of L-type Ca^{2+} channels, Na^+/Ca^{2+} exchanger (NCX), and sarcoplasmic reticulum (SR) Ca^{2+} release (13, 17, 39). However, these concentrations of H_2O_2 are ~10- to 100-fold higher than those observed for the burst in ROS production during I/R.

There has been considerable interest in determining whether the effects of ROS at pathophysiological doses similar to those observed during I/R could lead to myocardial tissue damage. Utilizing cultured neonatal rat ventricular myocytes (NRVM) as an in vitro model,

Address for reprint requests and other correspondence: P. A. Lucchesi, Univ. of Alabama at Birmingham, Dept. of Physiology and Biophysics, 1918 University Blvd., MCLM-986, Birmingham, AL 35294-0005 (E-mail: lucchesi@physiology.uab.edu).

The costs of publication of this article were defrayed in part by the payment of page charges. The article must therefore be hereby marked "*advertisement*" in accordance with 18 U.S.C. Section 1734 solely to indicate this fact.

we (31) previously found that low doses of H_2O_2 (similar to those generated during I/R) cause contractile dysfunction, which was associated with activation of the Na^+/H^+ exchanger (NHE). Activity of NHE-1, the only NHE isoform in the myocardium (8), is low during normal physiological conditions. Increased NHE-1 activity during reperfusion after an ischemic episode, although protective against acidosis, paradoxically contributes to the subsequent myocardial injury. NHE-1 inhibition has been shown to protect the I/R myocardium (18).

The relationship among ROS, Ca^{2+} overload, and enhanced NHE-1 activity during I/R injury remains to be determined. One possibility is that the increased NHE-1 activity results in excess intracellular Na^+, leading to an alteration in the activity of the NCX, favoring Ca^{2+} accumulation within the cell (19). Thus NHE-1 could have deleterious effects on myocardial tissue during I/R by contributing to the Ca^{2+} overload in the cardiomyocyte.

The extracellular signal-regulated kinase 1/2 (ERK1/2) mitogen-activated protein kinases (MAPK) represent attractive candidate kinases for regulating NHE-1 in response to I/R and or ROS. ERK1/2 are activated during I/R in conscious rabbits (29), and H_2O_2 and hypoxia activate members of the MAPK family, including p38, c-*jun* NH_2-terminal kinase, and ERK1/2 (1, 23, 31). We have also shown that ERK1/2 are responsible for H_2O_2-stimulated NHE-1 activation in NRVM (31) and for NHE-1 phosphorylation in the I/R rat myocardium (26).

The present study investigates the role of ERK1/2 MAPK and NHE-1 in H_2O_2-induced Ca^{2+} overload in spontaneously beating NRVM. Short-term exposure to low levels of H_2O_2 (50 μM) caused a dramatic diastolic Ca^{2+} overload that was reduced by ERK1/2 inhibition and NHE-1 blockade. Our results are consistent with the hypothesis that H_2O_2 may cause Ca^{2+} overload in the cardiomyocyte partially through ERK1/2-mediated phosphorylation of NHE-1.

METHODS

Cell preparation and culture. Primary cultures of rat ventricular myocytes were obtained from 1- to 2-day-old Sprague-Dawley rats by enzymatic dissociation of ventricular tissue (32). Myocytes were further purified with differential preplatings for 5 min on collagen-coated plates. The remaining cells were then plated onto collagen-coated glass coverslips (Warner) in 12-well plates at a density of 1,600 per mm^2 in complete serum-free PC-1 medium (BioWhittaker) supplemented with antibiotic-antimycotic solution (GIBCO) and 10 μM arabinosidase C and cultured for 24 h at 37°C. These dense cultures beat spontaneously within 24 h and exhibit <10% contamination by nonmuscle cells. NVRM media was changed after 24 h and then maintained for 2–24 h in a 2:1 mixture of serum-free Dulbecco's modified Eagle's-Ham's F-12-PC-1 media supplemented with an antibiotic-antimycotic solution.

Measurement of intracellular Ca^{2+}. NVRM were loaded with 3 μM fura 2-acetoxymethyl ester in Tyrode basic salt solution (Sigma), supplemented with 0.1% bovine serum albumin for 20 min at 37°C, followed by a 30-min unloading period in Tyrode basic salt solution at room temperature, minimizing dye compartmentalization. The coverslip was placed on an inverted microscope (model IX50, Olympus) secured in an imaging chamber (Warner) and perfused with Tyrode basic salt solution for 5 min (with or without pharmacological inhibitors). This equilibration period was followed by 5 min of perfusion of Tyrode basic salt solution with 50 μM H_2O_2 and a subsequent 5- to 10-min washout period in Tyrode basic salt solution (with or without pharmacological inhibitors). For all inhibitor studies, the drug was used at the same concentration during the unloading, equilibration, H_2O_2 perfusion, and washout periods.

For each experiment, intracellular Ca^{2+} concentration ($[Ca^{2+}]_i$) was measured in 5–10 cells. Cell fluorescence was measured using alternating excitation wavelengths (340 and 380 nm) controlled by a Spectromaster monochromatic light source (Olympus). Video images of fluorescence at 510-nm emissions were obtained using a LSR AstroCam CCD camera (Olympus) and the digitized measurement of emitted fluorescence was recorded using Merlin for Windows software (Olympus). The autofluorescence of unloaded myocytes was negligible compared with the fura 2-loaded myocytes and therefore was not subtracted. R_{max} (fluorescence ratio at saturating Ca^{2+}) and R_{min} (fluorescence ratio at 0 Ca^{2+}) were determined empirically at the end of each experiment by treating cells with 10 μM ionomycin in a $CaCl_2$ containing solution or with 10 mM EGTA in nominally Ca^{2+}-free solution, respectively. The equation $[Ca^{2+}]_i = K_d \times \beta(R - R_{min})/(R_{max} - R)$ (15) was used to construct a standard curve relating the fluorescence ratio to $[Ca^{2+}]_i$ for each experiment using the Merlin program. In this equation, the R value is the ratio of fluorescence with excitation at 340 and 380 nm, and β is the ratio of fluorescence with excitation at 380 nm in 0 Ca^{2+} to that saturating Ca^{2+}. K_d is the effective dissociation constant for fura 2 and was used as 224 nM (4, 7, 20). The data were analyzed with Merlin software and graphed using Delta Graph version 4.5 software for Macintosh.

Measurement of intracellular pH. NRVMs were plated at a density of 3×10^6 cells per 35-mm dish containing two 9 × 22-mm collagen-coated glass coverslips. Forty-eight hours after being plated, the cells were loaded with 2′,7′-bis(2-carboxyethyl)-5(6)-carboxyfluorescein (BCECF) by incubation with BCECF-acetoxymethyl ester (2 μM), 1 mg/ml bovine serum albumin, and 0.02% Pluronic F127 in Tyrode basic salt solution (Sigma) for 15 min in the dark at room temperature. The cells were then washed three times with Krebs solution and incubated in Krebs solution and 5 μM HOE-642 for ~1 h in the dark before BCECF fluorescence was recorded. BCECF fluorescence was recorded using a Perkin-Elmer LS50B fluorescence spectrophotometer, as previously described (31). A ratio of fluorescence emitted at 515 nm from excitation at 490 nm to that at 440 nM was converted to intracellular pH using the nigericin high-K^+ protocol of Thomas et al. (36).

Preparation of cell lysates for MAPK experiments with Western blot analysis. Cell lysates (25 μg) were subjected to sodium dodecyl sulfate-polyacrylamide gel electrophoresis (SDS-PAGE) under reducing conditions and transferred to nitrocellulose (Hybond, Amersham). The blots were incubated for 1 h with primary antibody and 1 h with secondary antibody (horseradish peroxidase-conjugated anti-rabbit IgG). Immunoreactive bands were visualized with the use of enhanced chemiluminescence (Amersham). Autoradiograms were scanned with an AFGA scanner and densitometric analysis performed with NIH Image version 1.6.

In-gel kinase assay. NHE-1 kinase activity and MAPK activity were analyzed by the in-gel kinase assay as de-

scribed previously (37). Cell lysates (30 μg) were fractionated by SDS-PAGE in a gel in which 0.15 mg/ml of NHE-1 fusion protein [amino acids 639–815 of NHE-1 coupled to glutathione *S*-transferase (GST)] had been copolymerized. The phosphorylation assay was performed by placing the gel in 10 ml of buffer containing 50 μM ATP with 100 μCi [γ-^{32}P]ATP and incubating for 1 h at 30°C. The reaction was terminated by immersion of the gel in a fixative solution (5% trichloroacetic acid and 10 mM sodium pyrophosphate). The radioactivity was quantified by densitometric analysis of scanned images.

Data analysis. Data were analyzed using InStat statistical software (GraphPad). All results are expressed as means ± SE. One-way analysis of variance with Dunnett's posttest was used to compare control versus treated groups. Differences between groups were considered statistically significant at $P < 0.05$.

RESULTS

H_2O_2 causes diastolic $[Ca^{2+}]_i$ overload in NRVM. We (31) reported that exposure of spontaneously beating NRVM to low concentrations of H_2O_2 resulted in a sustained decrease in contractility. To determine whether this contractile dysfunction was associated with intracellular Ca^{2+} overload, we examined the effects of H_2O_2 on diastolic $[Ca^{2+}]_i$. Acute exposure to low levels of H_2O_2 caused a profound increase in diastolic $[Ca^{2+}]_i$ during the washout period, similar to the Ca^{2+} overload observed during I/R. Compared with baseline, exposure to 50 μM H_2O_2 for 5 min led to a significant 1,210 ± 325 nM (from 74.8 ± 43.7 to 1,280 ± 314 nM) increase in diastolic $[Ca^{2+}]_i$ during the subsequent 10-min washout period (Fig. 1). NRVM responded to H_2O_2 with both a time- and dose-dependent increase in resting $[Ca^{2+}]_i$ during washout. A significant alteration in Ca^{2+} overload was detected during washout after a 2.5-min exposure to 50 μM H_2O_2 (273 ± 97 nM, $P < 0.05$) and was maximum at 5 min (Fig. 1*B*). As shown in Fig. 1*C*, H_2O_2 elicited a concentration-dependent diastolic Ca^{2+} overload on washout that was observed at 10 μM, significant at 25 μM (584 ± 179 nM, $P < 0.05$) and maximum at 50 μM H_2O_2.

Involvement of NHE-1 and ERK1/2 MAPK in H_2O_2-induced diastolic Ca^{2+} overload. We have previously demonstrated that H_2O_2 activates NHE-1 in an ERK1/2 MAPK-dependent manner. To link these

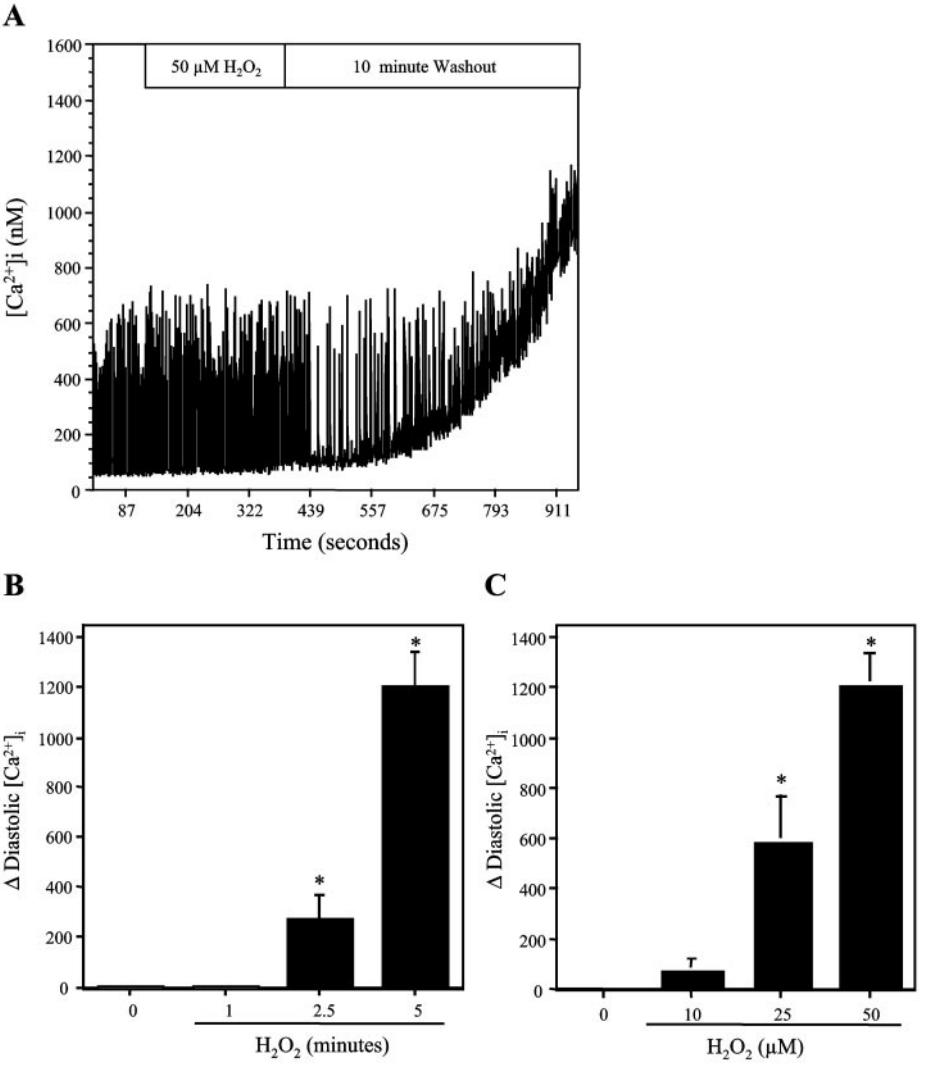

Fig. 1. H_2O_2 induced increases in diastolic intracelluar Ca^{2+} concentration ($[Ca^{2+}]_i$) during washout. Fura 2-loaded, spontaneously beating neonatal rat ventricular myocytes (NRVM) were perfused with H_2O_2 in Tyrode basic salt solution for 5 min, followed by a 10-min washout period in Tyrode basic salt solution alone. Change in diastolic $[Ca^{2+}]_i$ was calculated as the difference between the beginning and the end of washout with Tyrode basic salt solution (10 min) after H_2O_2 perfusion. *A*: representative trace with 50 μM H_2O_2 for $n = 10$ experiments. *B*: time-dependent changes in $[Ca^{2+}]_i$. Cumulative results from $n = 4$ experiments. *C*: concentration-dependent changes in diastolic $[Ca^{2+}]_i$. Cumulative results from $n = 4$ experiments. *$P < 0.05$ compared with control.

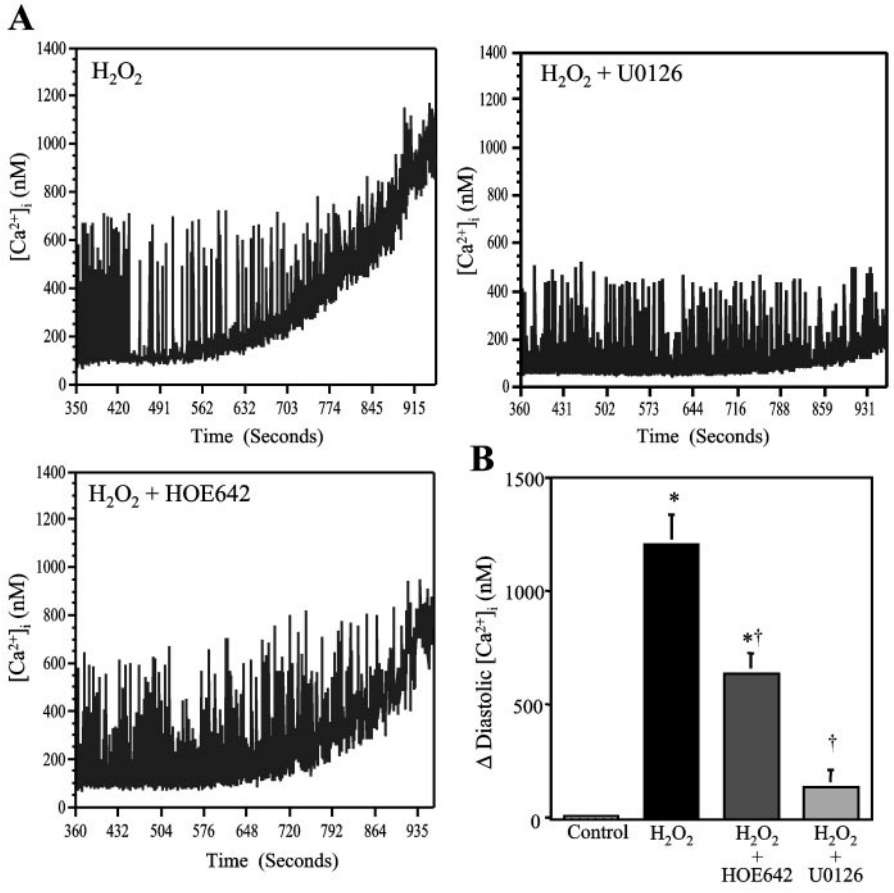

Fig. 2. Effects of inhibitors of the extracellular signal-related kinase 1/2 (ERK1/2) mitogen-activated protein kinase (MAPK) and Na^+/H^+ exchanger-1 (NHE-1) on H_2O_2-induced increase in diastolic $[Ca^{2+}]_i$. Fura 2 loaded NRVM were pretreated with no inhibitor (H_2O_2 alone), ERK kinase (MEK) inhibitor (5 μM U-0126), or NHE-1 inhibitor (5 μM HOE-642) for 30 min. Inhibitors were used to pretreat the cells during the 30-min unloading of fura 2 and were present throughout the duration of the experiment. Change in diastolic $[Ca^{2+}]_i$ was calculated as the difference between the beginning and the end of washout with Tyrode basic salt solution (10 min) following H_2O_2 perfusion. *A*: representative traces during a 10-min washout in Tyrode basic salt solution. *B*: cumulative data from $n = 5$ experiments. *$P < 0.05$ compared with control; †$P < 0.05$ compared with H_2O_2 alone.

events to H_2O_2-induced diastolic Ca^{2+} overload, we examined the effects of the NHE-1 blocker HOE-642 and the ERK kinase (MEK) inhibitor U-0126 on H_2O_2-induced increases in resting $[Ca^{2+}]_i$ (Fig. 2*A*). The concentrations of the inhibitors used were based on preliminary experiments that determined the minimal effective concentration that blocked H_2O_2-induced NHE-1 activity and ERK1/2 activation, respectively (data not shown). Pretreatment with HOE-642 (5 μM) led to a 50% reduction (from 1,208 ± 132 to 639 ± 92 nM, $P < 0.05$) in H_2O_2-induced diastolic Ca^{2+} overload (Fig. 2*B*). To confirm that this concentration of HOE-642 blocked NHE-1 activity, we examined its effects on H_2O_2-induced, Na^+-dependent recovery from an acid load in spontaneously beating NRVM. As shown in Fig. 3, NRVM treated with 50 μM H_2O_2 in the absence of pharmacological inhibitors exhibited complete recovery from an acid load. Treatment with HOE-642 completely abolished NHE-1 activity. These results are consistent with HOE-642 blunting H_2O_2-induced diastolic Ca^{2+} overload secondary to NHE-1 inhibition.

We then examined the involvement of the ERK1/2 MAPK pathway in diastolic Ca^{2+} overload and NHE-1 activation in response to H_2O_2. Treatment with the MEK inhibitor U-0126 (5 μM) resulted in an 88% decrease in the rise in diastolic Ca^{2+} levels after H_2O_2 treatment. Similar to our previous study (31) with the MEK inhibitor PD-90859, U-0126 (5 μM) blocked

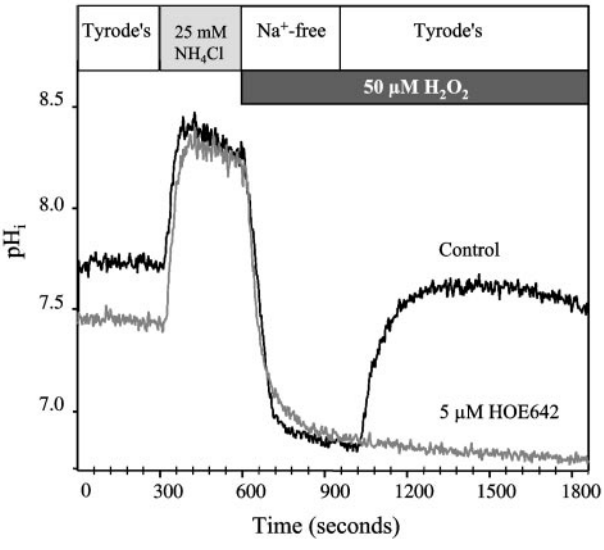

Fig. 3. HOE-642 blocks Na^+-dependent pH recovery from an acid load. Intracellular pH (pH_i) was measured with 2′,7′-bis(2-carboxyethyl)-5(6)-carboxyfluorescein (BCECF) in NRVM during exposure to NH_4Cl (25 mM, light gray box), followed by removal of external Na^+ (to induce an acid load) and reintroduction of Na^+ (Tyrode basic salt solution). The latter two solutions also contained 50 μM H_2O_2. Experiments were conducted in the absence (Control) or presence of 5 μM HOE-642 (cells were pretreated with 5 μM HOE-642 for 48 min before recording began and the drug was present in all solutions). Recovery from the acid load in the presence of Na^+ is an indication of NHE activity. Results are representative of 3 independent experiments.

H_2O_2-stimulated recovery from an acid load (data not shown). U-0126 also caused a dose-dependent decrease in H_2O_2-stimulated ERK1/2 phosphorylation, with complete inhibition at concentrations ≥2.5 μM (Fig. 4*A*).

To gain insight into the mechanisms by which ERK1/2 MAPKs mediate the activation of NHE-1 by H_2O_2, we examined the ability of ERK1/2 to phosphorylate NHE-1 using in-gel kinase assays with the carboxycytoplasmic tail of NHE-1 (amino acids 639–815) coupled to GST. Exposure to 100 μM H_2O_2 led to a significant increase in NHE-1 phosphorylation by proteins that correspond to ERK1 (44 kDa), ERK2 (42 kDa), and 90-kDa ribosomal S6 kinase ($p90^{rsk}$) (Fig. 4*B*). Both NHE-1 phosphorylation and ERK1/2 activation by H_2O_2 were significantly blocked (~85%) by 5 μM U-0126. In a series of separate experiments, U-0126 also blocked H_2O_2-induced $p90^{rsk}$ phosphorylation (data not shown). On the other hand, the p38 MAPK inhibitor SB-203580 (10 μM), a concentration that completely inhibits H_2O_2-induced p38 MAPK activation (data not shown), was without effect. Together, these data show that ERK1/2 MAPK phosphorylate NHE-1 and activate NHE-1 activity in vitro.

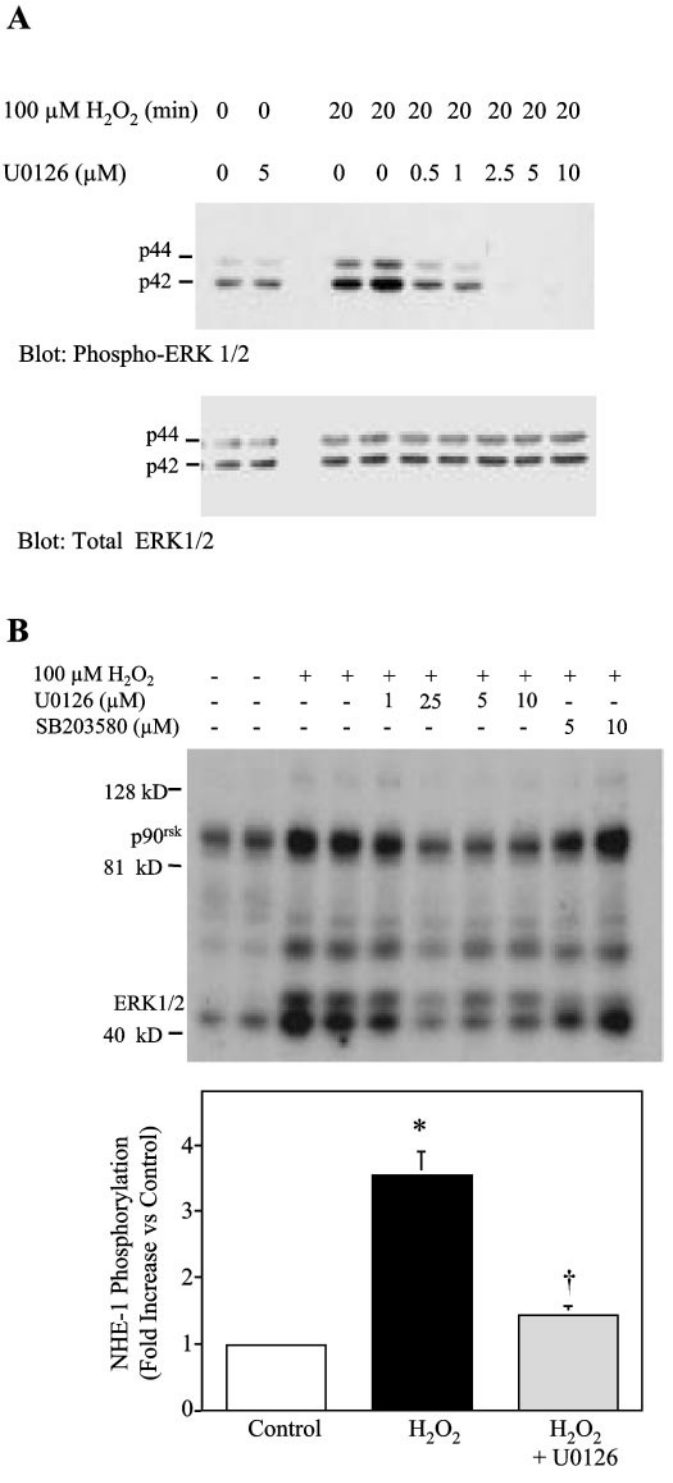

Fig. 4. H_2O_2-induced ERK1/2 activation and NHE-1 phosphorylation are blocked by MEK inhibition. Cultured NRVM were treated with H_2O_2 for 20 min ± pretreatment for 45 min with U-0126. *A*: Western blot analysis was performed with anti-phospho-ERK1/2 antibodies (1:2,000, *top*) or total ERK1/2 antibodies (1:3,000, *bottom*). Representative blots of $n = 3$ experiments. *B*: in-gel kinase assay using 0.15 mg/ml of NHE-1 fusion protein [amino acids 501–815 of NHE-1 coupled to glutathione *S*-transferase (GST)] as a substrate. *Top*: representative blot; *bottom*: cumulative data from $n = 3$ experiments. *$P < 0.01$ vs. control; †$P < 0.01$ vs. H_2O_2.

DISCUSSION

It is widely accepted that reperfusion of ischemic myocardium leads to contractile dysfunction and injury. Although the pathogenesis of this injury is complex, Ca^{2+} overload, ROS, and the NHE-1 have been implicated as key mechanisms that are responsible for the deleterious effects of I/R. The goal of the present study was to further elucidate the mechanisms that link ROS to altered Ca^{2+} homeostasis in cardiac myocytes. Previously, our laboratory (31, 37) showed H_2O_2-induced activation of MAPKs, increased NHE-1 activity, and decreased contractility in NRVM and adult RVM. The results from the current study provide direct evidence that low concentrations of H_2O_2 caused a significant diastolic Ca^{2+} overload that was reduced by NHE-1 blockade and abolished by MEK inhibition. This is the first evidence that directly links low levels of H_2O_2 to increases in cardiomyocyte resting $[Ca^{2+}]_i$ through NHE-1 activation.

There are several functional alterations in Ca^{2+} homeostatic proteins that could contribute to the H_2O_2-induced Ca^{2+} overload. These mechanisms include increased Ca^{2+} influx through voltage-sensitive Ca^{2+} channels (either direct modulation of channel activity or indirect through inhibition of K^+ channels and subsequent membrane depolarization), enhanced SR Ca^{2+} release, inhibition of Ca^{2+} uptake by the SR Ca^{2+} ATPase, or enhanced Na^+/Ca^{2+} exchange through direct modulation of the NCX or indirect activation secondary to increased NHE-1 activity. Our data are most consistent with the indirect modulation of Na^+/Ca^{2+} exchange secondary to NHE-1 activation. The following lines of evidence support this contention. First, we have previously shown that low concentrations of H_2O_2 increase NHE-1 activity in NRVM. Second, this study demonstrates that H_2O_2-induced Ca^{2+} overload was

significantly inhibited by NHE-1 blockade with HOE-642 at a concentration that completely blocks NHE-1 activity (Figs. 2 and 3). The results indicating that NHE-1 contributes to the Ca^{2+} overload that occurs in response to oxidative stress are in close agreement with previous studies (19, 38) that have demonstrated the crucial relationship between NHE activation, NCX modulation, and the development of cardiomyocyte Ca^{2+} overload. However, we cannot rule out a direct modulation of NCX by H_2O_2 because HOE-642 did not completely block H_2O_2-induced Ca^{2+} overload at concentrations that completely inhibited H_2O_2-induced, Na^+-dependent recovery from an acid load. This possibility is supported by a recent report (33) demonstrating that direct activation of the reverse mode of NCX contributes to reoxygenation-induced cardiomyocyte injury and altered Ca^{2+} flux. In addition, a recent report (13) shows that high concentrations of H_2O_2 activate the reverse mode of NCX in guinea pig ventricular myocytes. Taken together, these results suggest that H_2O_2 causes diastolic Ca^{2+} overload by modulation of both NHE-1 and NCX.

Our results are in close agreement with the concept that specific NHE-1 inhibitors exert beneficial effects on recovery from I/R injuries and diminish post-I/R Ca^{2+} overload. Early studies (18, 27) demonstrated that amiloride or its derivatives reduce Na^+/Ca^{2+} loading and enhance postischemic myocardial recovery. These inhibitors, however, are known to affect other sarcolemmal proteins, including NCX (11). Newer, more specific NHE-1 inhibitors have been shown to reduce myocardial damage after I/R injury that is characterized by an improvement in the postischemic recovery of left ventricular developed pressure, decreases in creatine phosphate release, and a reduction in tissue Na^+ and Ca^{2+} content (5, 16, 24, 40).

To elucidate the mechanisms by which H_2O_2 regulates NHE-1 activity, we examined the effects of MEK inhibition with U-0126. We previously showed that activation of NHE-1 by H_2O_2 was dependent on ERK1/2 MAPKs (31). Using in-gel kinase assays, we showed that U-0126 inhibited at least three kinases that were able to phosphorylate the NHE-1 COOH tail: ERK1, ERK2, and $p90^{rsk}$ (Fig. 4*B*). Moor et al. (25, 26), Snabaitis et al. (34), and our laboratory (37) have shown an important role of ERK MAPKs in the regulation of NHE-1 activity in cardiovascular tissue in response to neurohormones, serum, and I/R. In addition to directly phosphorylating NHE-1, ERK1/2 MAPKs also participate in NHE-1 regulation indirectly through $p90^{rsk}$ because U-0126 also blocked $p90^{rsk}$-dependent NHE-1 phosphorylation. The identification of $p90^{rsk}$ as a NHE-1 kinase is similar to a report in vascular smooth muscle (28) and is in close agreement with recent data (26) that demonstrated NHE-1 phosphorylation by $p90^{rsk}$ in response to myocardial I/R injury. In fact, a recent study (22) indicated that although recombinant NHE-1 was a substrate for ERK1/2 and $p90^{rsk}$, the stoichiometry of phosphorylation observed for $p90^{rsk}$ was greater than that for ERK1/2. $p90^{rsk}$ has been shown to phosphorylate NHE-1 at Ser^{703} but the ERK1/2 site has not been identified (35). Therefore, it is likely that H_2O_2-stimulated NHE-1 activation involves phosphorylation by $p90^{rsk}$ and/or ERK1/2 MAPK pathway.

Although H_2O_2 activates p38 MAPK in NRVM, it is not a major regulator of NHE-1, because the p38 inhibitor SB-203580 had no effect on H_2O_2-induced NHE-1 phosphorylation. A recent report (12) ruled out the involvement of p38 MAPK in NHE-1 activation in a human fibroblast cell line in response to osmotic stress. In agreement, also found was a diminished or insignificant role of p38 in NRVM (26). In contrast, p38 was shown to be a negative regulator of NHE-1 in VSMC treated with angiotensin II (22). Another recent report (21) has shown that p38 can phosphorylate and activate the NHE-1 and induce alkalinization in some tissues, but these effects of p38 may be tissue specific or may vary with the isoform of p38 involved.

Our results also suggest that the ERK1/2 pathway makes a significant contribution to H_2O_2-induced diastolic Ca^{2+} overload independent of NHE-1 phosphorylation, because U-0126, but not HOE-642, completely inhibited H_2O_2-induced increases in resting Ca^{2+} levels (Fig. 2). This suggests that ERK1/2 can regulate other ion transporters independently of NHE-1. The possible targets for ERK1/2 that could contribute to the cytosolic Na^+ and Ca^{2+} load include the Na^+-K^+-$2Cl^-$ cotransporter, which is activated by α_1-adrenergic agonist in an ERK1/2-dependent mechanism in cardiac myocytes (2), or the Na^+-HCO_3^- cotransporter, which is coupled to muscarinic receptor activation by ERK1/2 in renal epithelial cells (30). We cannot rule out the possibility that ERK1/2 can directly modulate NCX or Na^+/K^+ pump activity that could also contribute to alterations in Ca^{2+} or Na^+ homeostasis. However, there is no evidence that ERK1/2 MAPKs actually regulate NCX through phosphorylation. Moreover, H_2O_2, albeit at high concentrations, actually increased NCX activity (13). On the basis of this study, one would predict that the MEK inhibitor U-0126 would actually

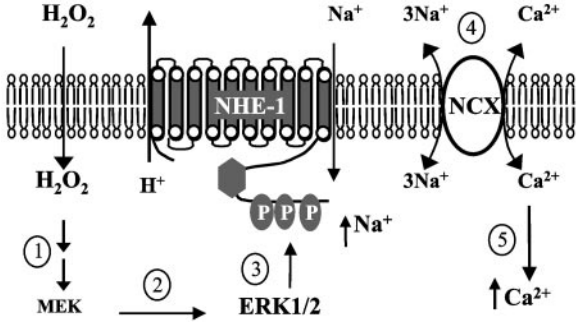

Fig. 5. Proposed link between H_2O_2 and diastolic Ca^{2+} overload in spontaneously beating NRVM, shown by the circled numbers. Exposure to H_2O_2 (similar to the increase in ROS during ischemia-reperfusion) results in the alteration of signaling proteins involved in the MAPK pathway, ultimately leading to MEK activation (1). MEK phosphorylates and activates ERK1/2 (2). ERK1/2 MAPK phosphorylate the COOH tail of NHE-1 increasing exchanger activity (3). The resulting rise in intracellular Na^+ alters NCX activity (4) leading to an increase in diastolic Ca^{2+} levels (5).

increase intracellular Ca^{2+} levels by eliminating the increase in forward mode of NCX.

On the basis of our results, we propose that H_2O_2-induced Ca^{2+} overload is primarily mediated by ERK1/2 MAPKs and partially through the phosphorylation and activation of NHE-1 (Fig. 5). The subsequent rise in intracellular Na^+ results in an inhibition of the forward mode and/or activation of reverse mode of NCX to ultimately cause a rise in intracellular Ca^{2+}. The diastolic Ca^{2+} overload may then contribute to the contractile dysfunction that is a hallmark of I/R injury. However, it is likely that other cellular processes participate in oxidative stress-induced myocardial contractile dysfunction. These mechanisms include alterations in excitation-contraction coupling, decreased myofilament sensitivity and/or responsiveness to Ca^{2+}, diminished mitochondrial function, and apoptosis. Further studies are needed to precisely define the signal transduction pathways that contribute to the altered cardiomyocyte function in response to ROS.

In conclusion, our results indicate that low levels of ROS cause a decrease in contractility and Ca^{2+} overload in NRVM. Therapies targeting ERK1/2 kinases and/or NHE-1 activation may ameliorate the alterations in Ca^{2+} homeostasis that contribute to myocardial tissue injury following I/R.

We thank Dr. Allen M. Samarel (Loyola University, Chicago, IL), for generously providing neonatal rat ventricular myocytes for pH measurements. We appreciate Dr. Mark Bevensee's insightful discussions and careful review of the manuscript. HOE-642 was a generous gift of Hoechst Marion Roussel.

This study was supported by National Heart, Lung, and Blood Institute Grants RO1-HL-63318 (to P. A. Lucchesi) and RO1-HL-60164 (to K. L. Byron), and the Heart and Stroke Foundation of Alberta (to L. Fliegel).

REFERENCES

1. **Aikawa A, Komuro I, Yamazaki Y, Zou Y, Kudoh S, Tanaka M, Shiojima I, Hiroi Y, and Yazaki Y.** Oxidative stress activates extracellular signal-regulated kinases through src and ras in cultured cardiac myocytes of neonatal rats. *J Clin Invest* 100: 1813–1821, 1997.
2. **Andersen GO, Enger M, Thoresen GH, Skomedal T, and Osnes JB.** α_1-Adrenergic activation of myocardial Na-K-2Cl cotransport involving mitogen-activated protein kinase. *Am J Physiol Heart Circ Physiol* 275: H641–H652, 1998.
3. **Bolli R.** Mechanism of myocardial "stunning." *Circulation* 82: 723–738, 1990.
4. **Borzak S, Kelly RA, Kramer BK, Matoba Y, Marsh JD, and Reers M.** In situ calibration of fura 2 and BCECF fluorescence in adult rat ventricular myocytes. *Am J Physiol Heart Circ Physiol* 259: H973–H981, 1990.
5. **Buerke M, Rupprecht HJ, vom Dahl J, Terres W, Seyfarth M, Schultheiss HP, Richardt G, Sheehan FH, and Drexler H.** Sodium-hydrogen exchange inhibition: novel strategy to prevent myocardial injury following ischemia and reperfusion. *Am J Cardiol* 83: 19G–22G, 1999.
6. **Buffon A, Santini SA, Ramazzotti V, Rigattieri S, Liuzzo G, Biasucci LM, Crea F, Giardina B, and Maseri A.** Large, sustained cardiac lipid peroxidation and reduced antioxidant capacity in the coronary circulation after brief episodes of myocardial ischemia. *J Am Coll Cardiol* 5: 633–639, 2000.
7. **Cheung JY, Tillotson DL, Yelamarty RV, and Scaduto RC Jr.** Cytosolic free calcium concentration in individual cardiac myocytes in primary culture. *Am J Physiol Cell Physiol* 256: C1120–C1130, 1989.
8. **Dyck JRB, Maddaford TG, Pierce GN, and Fliegel L.** Induction of expression of the sodium-hydrogen exchanger in rat myocardium. *Cardiovasc Res* 29: 203–208, 1995.
9. **Farber NE, Pieper GM, Thomas JP, and Gross GJ.** Beneficial effects of iloprost in the stunned myocardium. *Circ Res* 62: 204–215, 1988.
10. **Flitter WD.** Free radicals and myocardial reperfusion injury. *Br Med Bull* 49: 545–555, 1993.
11. **Floreani M and Luciani S.** Amiloride: relationship between cardiac effects and inhibition of Na^+/Ca^{2+} exchange. *Eur J Pharmacol* 105: 317–322, 1984.
12. **Gillis D, Shrode LD, Krump E, Howard CM, Rubie EA, Tibbles LA, Woodgett J, and Grinstein S.** Osmotic stimulation of the Na^+/H^+ exchanger NHE1: relationship to the activation of three MAPK pathways. *J Membr Biol* 181: 205–214, 2001.
13. **Goldhaber JI.** Free radicals enhance Na^+/Ca^{2+} exchange in ventricular myocytes. *Am J Physiol Heart Circ Physiol* 271: H823–H833, 1996.
14. **Goldhaber JI and Weiss JN.** Oxygen free radicals and cardiac reperfusion abnormalities. *Hypertension* 20: 118–127, 1992.
15. **Grynkiewicz G, Poenie M, and Tsien RY.** A new generation of Ca^{2+} indicators with greatly improved fluorescence properties. *J Biol Chem* 260: 3440–3450, 1985.
16. **Gumina RJ, Daemmgen J, and Gross GJ.** Inhibition of the Na^+/H^+ exchanger attenuates phase 1b ischemic arrhythmias and reperfusion-induced ventricular fibrillation. *Eur J Pharmacol* 396: 119–124, 2000.
17. **Josephson RA, Silverman HS, Lakatta EG, Stern MD, and Zweier JL.** Study of the mechanisms of hydrogen peroxide and hydroxyl free radical-induced cellular injury and calcium overload in cardiac myocytes. *J Biol Chem* 266: 2354–2361, 1991.
18. **Karmazyn M.** Amiloride enhances postischemic ventricular recovery: possible role of Na^+/H^+ exchange. *Am J Physiol Heart Circ Physiol* 255: H608–H615, 1988.
19. **Karmazyn M, Sostaric JV, and Gan XT.** The myocardial Na^+/H^+ exchanger: a potential therapeutic target for the prevention of myocardial ischaemic and reperfusion injury and attenuation of postinfarction heart failure. *Drugs* 61: 375–389, 2001.
20. **Kem DC, Johnson EI, Capponi AM, Chardonnens D, Lang U, Blondel B, Koshida H, and Vallotton MB.** Effect of angiotensin II on cytosolic free calcium in neonatal rat cardiomyocytes. *Am J Physiol Cell Physiol* 261: C77–C85, 1991.
21. **Khaled AR, Moor AN, Li A, Kim K, Ferris DK, Muegge K, Fisher RJ, Fliegel L, and Durum SK.** Trophic factor withdrawal: p38 mitogen-activated protein kinase activates NHE1, which induces intracellular alkalinization. *Mol Cell Biol* 21: 7545–7557, 2001.
22. **Kusuhara M, Takahashi E, Peterson TE, Abe J, Ishida M, Han J, Ulevitch R, and Berk BC.** p38 Kinase is a negative regulator of angiotensin II signal transduction in vascular smooth muscle cells: effects on Na^+/H^+ exchange and ERK1/2. *Circ Res* 83: 824–831, 1998.
23. **Laderoute KR and Webster KA.** Hypoxia/reoxygenation stimulates Jun kinase activity through redox signaling in cardiac myocytes. *Circ Res* 80: 336–344, 1997.
24. **Maddaford TG and Pierce GN.** Myocardial dysfunction is associated with activation of Na^+/H^+ exchange immediately during reperfusion. *Am J Physiol Heart Circ Physiol* 273: H2232–H2239, 1997.
25. **Moor AN and Fliegel L.** Protein kinase-mediated regulation of the Na^+/H^+ exchanger in the rat myocardium by mitogen-activated protein kinase-dependent pathways. *J Biol Chem* 274: 22985–22992, 1999.
26. **Moor AN, Gan XT, Karmazyn M, and Fliegel L.** Activation of Na^+/H^+ exchanger-directed protein kinases in the ischemic and ischemic-reperfused rat myocardium. *J Biol Chem* 276: 16113–16122, 2001.
27. **Murphy E, Perlman M, London RE, and Steenbergen C.** Amiloride delays the ischemia-induced rise in cytosolic free calcium. *Circ Res* 68: 1250–1258, 1991.
28. **Phan VN, Kusuhara M, Lucchesi PA, and Berk BC.** A 90-kD Na^+/H^+ exchanger kinase has increased activity in spontane-

ously hypertensive rat vascular smooth muscle cells. *Hypertension* 29: 1265–1272, 1997.

29. **Ping PP, Zhang J, Cao X, Li RCX, Kong D, Tang XL, Qiu Y, Manchikalapudi S, Auchampach JA, Black RG, and Bolli R.** PKC-dependent activation of p44/p42 MAPKs during myocardial ischemia-reperfusion in conscious rabbits. *Am J Physiol Heart Circ Physiol* 276: H1468–H1481, 1999.
30. **Robey RB, Ruiz OS, Baniqued J, Mahmud D, Espiritu DJ, Bernardo AA, and Arruda JA.** SFKs, Ras, and the classic MAPK pathway couple muscarinic receptor activation to increased Na-HCO_3 cotransport activity in renal epithelial cells. *Am J Physiol Renal Physiol* 280: F844–F850, 2001.
31. **Sabri A, Byron KL, Samarel AM, Bell J, and Lucchesi PA.** Hydrogen peroxide activates mitogen-activated protein kinases and Na^+/H^+ exchange in neonatal rat cardiac myocytes. *Circ Res* 82: 1053–1062, 1998.
32. **Samarel AM and Engelmann GL.** Contractile activity modulates myosin heavy chain-beta expression in neonatal rat heart cells. *Am J Physiol Heart Circ Physiol* 261: H1067–H1077, 1991.
33. **Schafer C, Ladilov Y, Inserte J, Schafer M, Haffner S, Garcia-Dorado D, and Piper HM.** Role of the reverse mode of the Na^+/Ca^{2+} exchanger in reoxygenation- induced cardiomyocyte injury. *Cardiovasc Res* 51: 241–250, 2001.
34. **Snabaitis AK, Hiroyuki Y, and Avkiran M.** Roles of mitogen-activated protein kinases and protein kinase C in alpha-1A adrenoceptor-mediated stimulation of the sarcolemmal Na^+/H^+ exchanger. *Circ Res* 86: 214–220, 2000.
35. **Takahashi E, Abe J, Gallis B, Aebersold R, Spring DJ, Krebs EG, and Berk BC.** $p90^{RSK}$ is a serum-stimulated Na^+/H^+ exchanger isoform-1 kinase. Regulatory phosphorylation of serine 703 of Na^+/H^+ exchanger isoform-1. *J Biol Chem* 274: 20206–20214, 1999.
36. **Thomas JA, Buchsbaum RN, Zimniak A, and Racker E.** Intracellular pH measurements in Erlich ascites tumor cells utilizing spectroscopic probes in situ. *Biochemistry* 81: 2210–2218, 1979.
37. **Wei S, Rothstein EC, Fliegel L, Dell'Italia LJ, and Lucchesi PA.** Differential MAP kinase activation and Na^+/H^+ exchanger phosphorylation by H_2O_2 in rat cardiac myocytes. *Am J Physiol Cell Physiol* 281: C1542–C1550, 2001.
38. **Xiao XH and Allen DG.** Role of Na^+/H^+ exchanger during ischemia and preconditioning in the isolated rat heart. *Circ Res* 85: 723–730, 1999.
39. **Xu KY, Zweier JL, and Becker LC.** Hydroxyl radical inhibits sarcoplasmic reticulum Ca^{2+}-ATPase function by direct attack on the ATP binding site. *Circ Res* 80: 76–81, 1997.
40. **Yamamoto S, Matsui K, Kitano M, and Ohashi N.** SM-20550, a new Na^+/H^+ exchange inhibitor and its cardioprotective effect in ischemic/reperfused isolated rat hearts by preventing Ca^{2+}-overload. *J Cardiovasc Pharmacol* 35: 855–862, 2000.
41. **Zweier JL, Flaherty JT, and Weisfeldt ML.** Direct measurement of free radical generation following reperfusion of ischemic myocardium. *Proc Natl Acad Sci USA* 84: 1404–1407, 1987.
42. **Zweier JL, Kuppusamy P, Williams R, Rayburn BK, Smith D, Weisfeldt ML, and Flaherty JT.** Measurement and characterization of postischemic free radical generation in the isolated perfused heart. *J Biol Chem* 264: 18890–18895, 1989.